J. of Supercritical Fluids 55 (2011) 955–962

Contents lists available at ScienceDirect

The Journal of Supercritical Fluids

journal homepage: www.elsevier.com/locate/supflu

Purification of algal anti-tyrosinase zeaxanthin from *Nannochloropsis oculata* using supercritical anti-solvent precipitation

Chun-Ting Shen[a], Po-Yen Chen[a], Jia-Jiuan Wu[a,f], Tse-Min Lee[d], Shih-Lan Hsu[e], Chieh-Ming J. Chang[a,*], Chiu-Chung Young[b], Chwen-Jen Shieh[c]

[a] Department of Chemical Engineering, National Chung Hsing University, 250, Kuo-Kuang Road, Taichung 402, Taiwan, ROC
[b] Department of Soil and Environmental Sciences, National Chung Hsing University, 250, Kuo-Kuang Road, Taichung 402, Taiwan, ROC
[c] Biotechnology Center, National Chung Hsing University, 250, Kuo-Kuang Road, Taichung 402, Taiwan, ROC
[d] Institute of Marine Biology, National Sun Yat-Sen University, No. 70, Lienhai Road, Kaohsiung 804, Taiwan, ROC
[e] Education and Research Department, Taichung Veterans General Hospital, 160, Taichung Harbor Road, Taichung 407, Taiwan, ROC
[f] Department of Nutrition, China Medical University, No. 91, Hsueh-Shih Road, Taichung 404, Taiwan, ROC

ARTICLE INFO

Article history:
Received 30 August 2010
Received in revised form
30 September 2010
Accepted 1 October 2010

Keywords:
Nannochloropsis oculata
Zeaxanthin
Elution chromatography
Submicrosize particles
Supecritical anti-solvent precipitation

ABSTRACT

This work investigated the changes in content of algal zeaxanthin in submicronized precipitates generated from the supercritical anti-solvent (SAS) process of extracting microalgae *Nannochloropsis oculata*. Following a reverse phase elution chromatography, the particulates were successfully generated from feed solutions containing zeaxanthin that ranged from 0.4 to 0.8 mg/mL by a SAS process. The precipitation condition was set at 323 K and pressures ranged from 10 to 20 MPa. Experimental results of a three-factor center composite response surface method for the SAS process indicated that the size of the precipitates was significantly affected by the flow rate of carbon dioxide. The purity of zeaxanthin increased with increasing solvent flow rate and with reducing solution concentration. The recovery of zeaxanthin and the morphology of the precipitates was also examined. The content of zeaxanthin in submicronsized precipitates increased from 485.9 (48.6%) to 673.7 mg/g (67.4%). This work demonstrates that elution chromatography coupled with a SAS process is an environmentally benign method to recover anti-tyrosinase zeaxanthin from *Nannochloropsis oculata* as well as to generate submicrosized precipitates of the purest zeaxanthin from algal solutions.

1. Introduction

Zeaxanthin ($C_{40}H_{56}O_2$) is the principal pigment obtained from yellow corn or from the marigold flower; it is involved in many important physiological functions of the human body. Dietary xanthophylls such as lutein and zeaxanthin play important roles against age-related macular degeneration (AMD) and other age-related eye disease (AED) [1–3]. Lutein and zeaxanthin have been found to accumulate in high concentrations within the human retina [4]. Photo-protective mechanisms are important to prevent harmful reactions in plants (marigold) and algae (*Nannochloropsis oculata*). Harmful reactions are induced by an excess of photons absorbed from sunlight irradiation. Carotenoids have been suggested as key molecules in these photo-protective mechanisms. For example, beta-carotene can act as an effective quencher of singlet oxygen in the photo-system II reaction center [5]. Another example, xanthophylls, especially zeaxanthin, is involved in the process of non-photochemical energy dissipation [6–10]. Algae or marigold containing zeaxanthin can be cultivated in the environment mentioned above. However, traditional organic solvent extraction of these thermal labile and light sensitive carotenoids from natural material is not so efficient due to low recovery of the carotenoid by total vaporization of the solvent at high boiling point. Co-solvent modified supercritical carbon dioxide (SC-CO_2) extraction of lipids and carotenoids from microalgae; ultrasound water extraction of vitamins B from SC-CO_2 defatted rice bran; and SC-CO_2 extraction of cinnamic acid derivatives from propolis were recently investigated [11–13]. These supercritical fluids extraction showed that the SC-CO_2 is a green solvent in recovering valuable compounds from natural materials.

Supercritical anti-solvent (SAS) precipitation of solutes from a liquid phase solution has been extensively applied in pigment dispersion and pharmaceutical recrystallization to produce fine particles with high yield [14,15]. This SAS approach has also been utilized in the separation of bioactive compounds from natural materials, including flavonoids, ginkgolides, lycopene, carotenoids and phenolic acid derivatives [16–22]. Additionally, experimental

* Corresponding author. Tel.: +886 4 2285 2592; fax: +886 4 2286 0231.
E-mail address: cmchang@dragon.nchu.edu.tw (C.-M.J. Chang).

0896-8446/$ – see front matter © 2010 Elsevier B.V. All rights reserved.
doi:10.1016/j.supflu.2010.10.003

data on the phase equilibrium between SC-CO_2 and an organic solvent is important in understanding the supercritical anti-solvent (SAS) process as supercritical, superheated, liquid and the co-existing phases directly influence the morphology, size and distribution of particles [23–25]. Three dimensionless parameters, Reynolds number ($\rho VD/\mu$; ρ: density of the fluid, V: velocity, D: pipe diameter and μ: fluid viscosity), Webers number ($\rho V^2 D/\sigma$; ρ: density of the droplet, V: droplet impact velocity, D: droplet diameter and σ: surface tension of droplet) and super-saturation of solutes (S/S^*; S: transient solubility, S^*: equilibrium solubility) have been recognized as major parameters that govern the mechanism of particle formation associated with SAS precipitation by Rantakyla et al. [23]. Super-saturation of solutes in a high-pressure solution is important to generate micronized particles in a SC-CO_2 anti-solvent precipitation process. However, the transient high super-saturation of the solutes (e.g. 1.0×10^4) in such a high-pressure system that is mixed with SC-CO_2 is very difficult to be measured, reported earlier by Chang et al. [24]. This study investigated SAS precipitations of submicron-sized particles containing zeaxanthin from purified algal solutions. The effect of the operation parameters (i.e. pressure, feed concentration, CO_2 flow rate) on purity and recovery of zeaxanthin was based on a three-factor center composite response surface methodology and was examined to determine the optimization of the purity of zeaxanthin in the SC-CO_2 precipitates.

2. Materials and methods

2.1. Materials

Nannochloropsis oculata was cultivated by sea water in five of 5 tons open-type polypropylene tanks sparkled with air for 15 days. After sedimentation by alunite coagulation, high speed centrifugal collection and freeze dried treatment, 500 g of algae in dry basins were donated by GeneReach Biotech. Company (Central Science Park, Taichung, Taiwan). The dried microalgae were then collected by sieving it between 60 (250 μm) and 80 (177 μm) mesh stainless steel screens under dimmed light and stored in a freezer at 193 K before extraction.

2.2. Chemical and standards

Analytical grade solvents used for the extractions, SAS processes, column chromatography and fractionations contained 99% ethanol (Mallinckrodt, USA), 99.5% acetone (Mallinckrodt, USA), 99.5% dichloromethane (DCM) (Mallinckrodt, USA). HPLC grade solvents used for the mobile phase in HPLC contained 99.5% methanol (Mallinckrodt, USA), 99.5% methyl tert-butyl ether (Mallinckrodt, USA). Ultrapure water (>18 M) was obtained using the Ultrapure™ water purification system (Louton Co., Ltd., Taipei, Taiwan) and was filtered through a 0.45 μm membrane filter prior to use. The analytical grade of F_{254} Silica-gel 60 resin (Merck, Germany) was purchased and used without further purification. And 99.95% CO_2 (Toyo gas, Taiwan) was used for SAS precipitation.

The authentic standards for carotenoids contained 90.0% lutein (Fluka, Switzerland), >95% zeaxanthin (Fluka, Switzerland), 95% β-cryptoxanthin (Sigma–Aldrich, USA), 95% trans-β-apo-8′-catotenal (Fluka, Switzerland), 95% mix isomers of β-carotene:α-carotene = 2:1 (Sigma–Aldrich, USA).

The reagents used for agar-plate tyrosinase inhibition included agar (Amresco, USA), 99.5% dimethyl sulfoxide (DMSO), sodium phosphate (Na_2HPO_4, NaH_2PO_4), 99% potassium phosphate (KH_2PO_4), mushroom tyrosinase, 3,4-dihydroxy-L-phenylalanine (L-Dopa), vitamin C (Sigma, USA), 2-phenoxyethanol (Sigma–Aldrich, USA), and No. 2 filter paper (Advantec, Japan).

2.3. Soxhlet extractions of Nannochloropsis oculata

Freeze-dried microalgal powders (10.5 g) were extracted using four different solvents separately over 16 h in a 175 mL Soxhlet extractor. After extraction, solvents were removed under vacuum and then weighed individually. The extracts were stored in a 193 K refrigerator before column chromatography was performed. All extractive and quantitative procedures were carried out under dimmed light.

2.4. Column chromatography and fractionation

The freeze-dried microalgae (50.0 g) were exhaustively extracted in dichloromethane with a 300 mL Soxhlet extractor. The algal extracts were concentrated under vacuum to yield a loading sample (3.6 g) for column chromatography. The loading sample was dissolved in mixed solvents of ethyl acetate (EA) and *n*-hexane (1:3, volume ratio). The solution was subjected to a 10 cm (ID) × 30 cm (L) glass column which was packed with silica gel as a stationary phase. The feed solution was just introduced on the top of silica gel layer by a positive displacement membrane pump. A similar experimental facility was described in detail in our previous study [25]. Isocratic elution was carried out using EA and *n*-hexane (1:3, volume ratio) at the flow rate of 7 mL/min. Finally, a total of 32 volume fractions were collected, and the solvent of each fraction was removed under vacuum and then weighed individually. The fractions were collected according to each 10 mL of eluted solution. The purified samples were stored in a 193 K refrigerator before HPLC analysis and SC-CO_2 precipitation.

2.5. The SC-CO_2 precipitation process

For interpretation of the schematic flow diagram of SC-CO_2 precipitation, the reader is referred to the study of the Chen et al. [12]. Liquid CO_2 was compressed using a high-pressure pump (*Spe-ed* SFE, Applied Separations, USA) (4) into the first surge tank (75 mL, $L/D = 30$) (8). It entered a second surge tank (750 mL, $L/D = 10$) (11) at a constant flow rate after it was preheated using a heat exchanger (7). Then, CO_2 flowed (18, 36, 54 g/min) through a metering valve (SS-31RS4-A, Swagelok, USA) (6–3) into a visible precipitator (TST, Taiwan) (12), and various concentrations (0.4, 0.6, 0.8 mg/mL) of feed solutions were delivered into the precipitator at a constant flow rate of 2 mL/min via a high-pressure liquid pump (L-6200A, Hitachi, Japan) (17). A coaxial nozzle of 0.007 in. inside diameter was installed in the entrance of the precipitator to spray off the feed solution. A stainless frit (37 μm) and an online filter (0.45 μm) were placed at the bottom of precipitator to prevent the penetration of particles. The operating pressure (10, 15, 20 MPa) was regulated using a back-pressure regulator (26-1722, Tescom, USA) (9–3), and the operating temperature (313 K) was controlled using a water bath circulator (5–3). The consumption of CO_2 was measured using a drum type gas meter (TG10/5, Ritter, Germany) (16).

2.6. Quantification of zeaxanthin

High-performance liquid chromatography (HPLC) was performed using a Hitachi 2130 pump and 2400 UV series system (Hitachi, Ltd., Tokyo, Japan). The analysis was carried out with a reverse-phase YMC C-30 (5 μm, 250 mm × 4.6 mm i.d.) and a Phenomenex Luna security guard cartridge C-18 (5 μm, 4 mm × 2.0 mm i.d.). The microalgal extracts were eluted using mobile phases of water (A) methanol (B) and methyl t-butyl ether (C). The eluent flow rate was maintained at 1 mL/min, the injection volume was 20 μL, and the detection wavelength and column temperature were set to 450 nm and 303 K. The elution gradients were as follows: 0 min, 10% A, 90% B, 0% C; 5 min, 4% A, 81% B, 15% C; 25 min, 4% A, 81% B,

Table 1
Experimental data concerning Soxhlet extractions of carotenoids from 10 g of *N. oculata* powder.

Entry	Solvent	TY (%)	C_{zea} (mg/g)	W_{zea} (mg/g)	R_{zea} (%)	C_{CAR} (mg/g_{ext})	W_{CAR} (mg/g_{alga})	R_{CAR} (%)
1	CH_2Cl_2	8.91	20.10	1.79	100	25.15	2.24	100
2	*n*-Hexane	5.33	19.59	1.04	58.1	25.67	1.37	61.2
3	EtOH	23.33	7.55	1.76	98.3	8.49	1.98	88.4
4	Toluene	10.70	9.99	1.07	59.8	12.44	1.33	59.4

TY: total yield of extract = $(W_{ext}/W_{feed.}) \times 100\%$; C_{zea}: concentration of zeaxanthin in extract; W_{zea}: the amount of zeaxanthin in microalgae; R_{zea}: recovery of zeaxanthin = $(W_{zea}/1.79) \times 100\%$; C_{CAR}: concentration of carotenoids in extract; W_{CAR}: the amount of carotenoids in microalgae; R_{CAR}: recovery of carotenoids = $(W_{CAR}/2.24) \times 100\%$.

15% C; 50 min, 4% A, 31% B, 65% C. The identity of zeaxanthin was confirmed by comparing its HPLC retention time with the analytical standards at the wavelength of 450 nm.

2.7. Analysis of particle size distribution and morphology

The mean particle size and particle size distribution (PSD) were determined using a light scattering particle size analyzer (Beckman Coulter, Counter F5, USA). The morphologies of the precipitates were examined using a field emission scanning electron microscope (FESEM) (UltraPlus series, Zeiss, GE). The precipitates were sputtered with a layer of platinum film and the FESEM images were observed under a voltage of 2 kV.

2.8. Agar-plate tyrosinase inhibition

The whitening tests were performed using mushroom tyrosinase (200 Unit/mL) that was smeared on an agar plate that contained 97.5% distilled water, 0.1% L-Dopa, 2% agar and 0.4% 2-phenoxyethanol. The samples at certain concentrations were loaded on the surface of a piece of No. 2 filter paper which was placed on the agar-plate and then incubated at room temperature for 6 h. The bright area of the sample represents the area of tyrosinase inhibition.

3. Results and discussion

3.1. HPLC analysis of carotenoids

Fig. 1 shows the HPLC chromatograms for the analysis of carotenoids from the extracted, fractionated and precipitated samples. From Fig. 1(b), carotenoids from Soxhlet dichloromethane (DCM) extraction were separated successfully using a C30 column with a gradient elution method. Each carotenoid was identified by comparing it with its commercial standard chromatogram as shown in Fig. 1(a). The amount of zeaxanthin was higher than

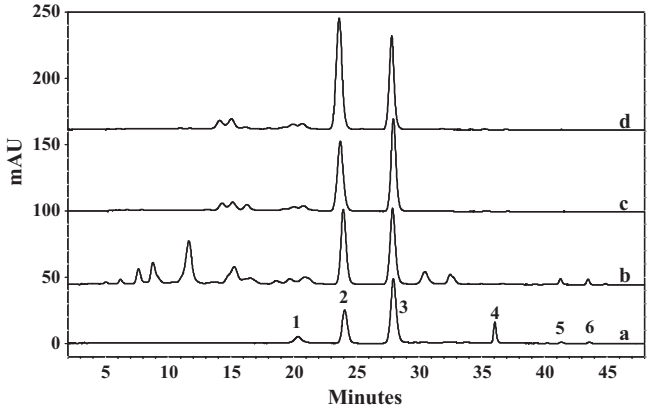

Fig. 1. HPLC chromatogram of algal samples and standards (a) STDs; (b) SOX-CH_2Cl_2; (c) column partition fractions; (d) SAS precipitates. (1, lutein; 2, zeaxanthin; 3, internal standard; 4, β-cryptoxanthin; 5, α-carotene; 6, β-carotene).

Table 2
Experimental data on column partition fractionation of algal extract.

Entry	$W_{collected}$ (mg)	C_{zea} (mg/g)	R_{zea} (%)
F1–F22	2270.5	0	0
F23	23.5	121.2	3.9
F24	12.0	348.2	5.8
F25	9.8	443.1	6.0
F26	10.5	468.3	6.8
F27	11.0	462.1	7.0
F28	9.3	522.4	6.7
F29	8.7	530.9	6.4
F30	10.8	484.6	7.2
F31	10.3	462.3	6.6
F32	11.2	252.8	3.9
$\sum_{24}^{32}$	93.6	436.2	56.4

W_{feed}: 3600 mg; C_{feed}: 20.1 mg/g_{ext}; eluent: *n*-hexane:ethyl acetate = 3:1; $W_{collected}$: weight of each fraction; C_{zea}: concentration of zeaxanthin in each fraction; R_{zea}: recovery of zeaxanthin = $(W_{collected} \times C_{zea})/(3600 \times 20.1) \times 100\%$.

other carotenoids in the sample of Soxhlet DCM extraction. The chromatogram of the sample after column partition is shown in Fig. 1(c). The result reveals that the concentrations of cartenoides decreased after the column partition except for zeaxanthin. Finally, Fig. 1(d) shows that the amount of zeaxanthin further increased after undergoing the process of supercritical anti-solvent precipitation. The purity of zeaxanthin increased from the Soxhlet extract, to the column fractions, and finally to the SAS precipitates stepwise.

3.2. Efficiency of Soxhlet extraction

Table 1 represents total yield (TY), concentrations of zeaxanthin (C_{zea}), and recovery of zeaxhanthin (R_{zea}). The definitions of these items are shown as follows:

$$TY = \left[\frac{\text{weight of the extract}}{\text{weight of feed material}}\right] \times 100\%$$

$$C_{zea} = \left[\frac{\text{weight of zeaxanthin in the extract}}{\text{weight of algal extract}}\right]$$

$$R_{zea} = \left[\frac{\text{weight of zeaxanthin in the extract}}{\text{weight of zeaxanthin in algae}}\right]$$

Organic solvents are frequently used to extract carotenoids from natural products. In our previous study, Soxhlet dichloromethane (DCM) extraction was used to recover zeaxanthin from the algae, and four extraction times (4, 8, 12, 16 h) were tested [11]. The

Table 3
Solubility data of algal extracts dissolved in different solvents.

	EtOH (mg/mL)	Acetone (mg/mL)	Dichlolomethane (mg/mL)
93% Zea	0.10	0.87	8.51
40% Zea	0.65	1.04	10.46
29% Zea	1.00	2.11	11.31
13% Zea	2.58	4.57	13.73

Table 4
RSM-designed SC-CO_2 antisolvent precipitation at 313 K.

SEM #	P (MPa)	P (bar)	C_{feed} (mg/mL)	Q_{CO_2} (g/min)	C_{zea} (mg/g)	TY (%)	R_{zea} (%)
1(F)	10	100	0.4	18	486.3	68.3	76.1
2(A)	10	100	0.6	36	578.4	64.8	85.9
3(F)	10	100	0.8	18	485.9	80.1	89.2
4(A)	10	100	0.8	54	653.2	58.6	87.8
5(F)	10	100	0.4	54	561.1	62.8	80.8
6(A)	15	150	0.6	54	673.7	58.1	89.7
7(C)	15	150	0.6	36	602.9	52.4	72.4
8(F)	15	150	0.4	36	660.7	55.4	83.9
9(A)	15	150	0.8	36	614.2	55.9	78.7
10(A)	15	150	0.6	18	597.3	61.0	83.5
11(A)	20	200	0.6	36	541.1	58.2	72.2
12(F)	20	200	0.8	18	544.4	65.3	81.5
13(F)	20	200	0.4	18	655.2	55.2	82.9
14(F)	20	200	0.4	54	622.3	51.8	73.9
15(F)	20	200	0.8	54	575.7	58.1	76.7

P: pressure of precipitator; C_{feed}: concentration of feed; Q_{CO_2} : flow rate of CO_2; TY: total yield of precipitates = $(W_{crystallization}/W_{feed}) \times 100\%$; C_{zea}: concentration of zeaxanthin in precipitates; R_{zea}: recovery of zeaxanthin = $(10 \times TY \times C_{zea}/1000)/(10 \times 436.2/1000) \times 100\%$; Q_{feed}: 2 mL/min; $C_{zea,feed}$ = 436.2 mg/g; W_{feed}: 10 mg weight of feed.

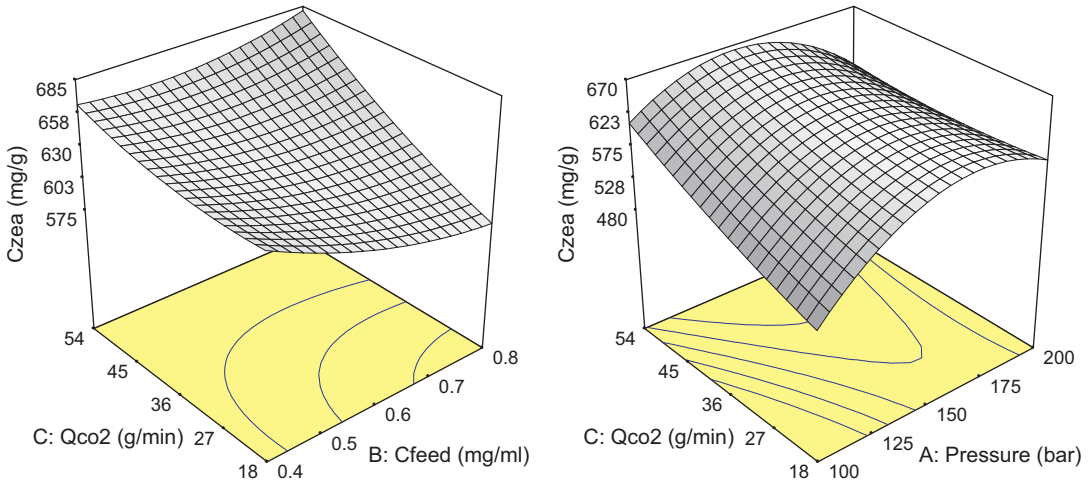

a Pressure= 15 MPa

b C_{feed} = 0.6 mg/ml

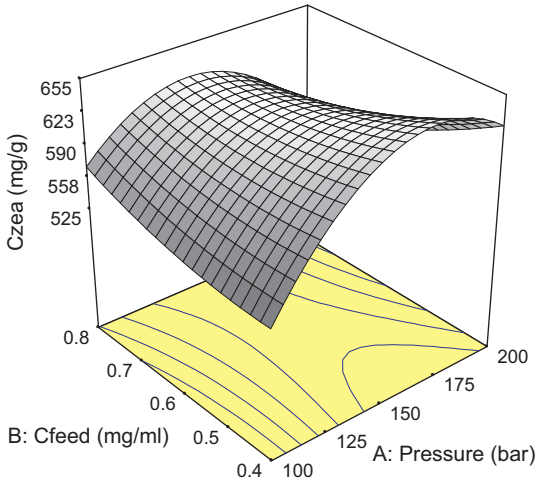

c Q_{co2}= 36 g/min

Fig. 2. Three-dimensional representation of the concentration of zeaxanthin (C_{zea}) (F-testing: R^2 = 0.91, S.D. = 29.43 mg/g). Center point: (a) pressure: 15 MPa; (b) C_{feed}: 0.6 mg/mL; (c) Q_{CO_2} = 36 g/min.

findings presented that after 16 h of extraction, the content of zeaxanthin in the microalgal extract reached the maximum value. Due to the fact that the difference between the 12 and 16 h data is very small, the maximum amount of 1.79 mg/g_{alga} was considered to be 100% recovery of zeaxanthin obtained by the 300 mL Soxhlet DCM extraction of 10 g of microalgae. In our experiment, three solvents (ethanol, toluene, *n*-hexane) were used to evaluate extraction efficiency of zeaxanthin compared to that of the dichloromethane, shown in Table 1. From the table it can be seen that the recovery of zeaxanthin was the highest value when extracted by DCM, but was close to ethanol (R_{zea} = 98%). The recovery of zeaxanthin decreased significantly with decreasing polarity of the solvents, and had no relationship to the boiling point of solvents. This phenomenon was caused by the higher solubility of zeaxanthin dissolved in ethanol and DCM than those of the other solvents.

3.3. Column chromatography fractionation

Compared to the solvent of Soxhlet extraction, the recovery of zeaxanthin in Soxhlet DCM is better than that of Soxhlet ethanol. Therefore, the Soxhlet DCM extract was adopted and further subjected to column chromatography to yield 32 fractions. A medium-pressure normal-phase column partition fractionation was adopted herein to purify zeaxanthin from the algal solution. Table 2 presents the concentration of zeaxanthin (C_{zea}) in each fraction. The fractions of 24–32 were identified as zeaxanthin-

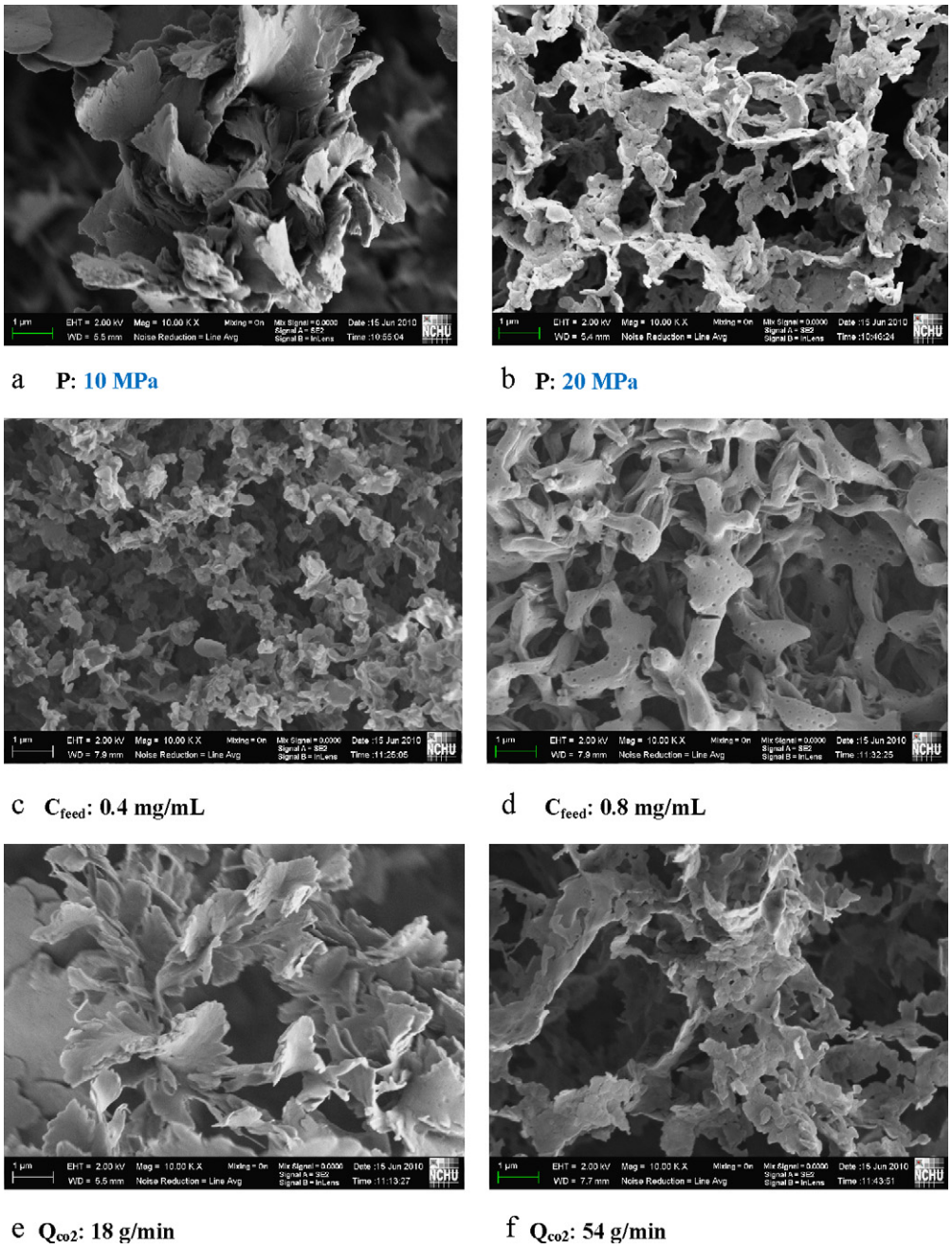

Fig. 3. FESEM images of precipitated algal samples at (a) *P*: 10 MPa, C_{feed}: 0.6 mg/mL, Q_{CO_2} = 36 g/min; (b) *P*: 20 MPa, C_{feed}: 0.6 mg/mL, Q_{CO_2} = 36 g/min; (c) *P*: 15 MPa, C_{feed}: 0.4 mg/mL, Q_{CO_2} = 36 g/min; (d) *P*: 15 MPa, C_{feed}: 0.8 mg/mL, Q_{CO_2} = 36 g/min; (e) *P*: 20 MPa, C_{feed}: 0.8 mg/mL, Q_{CO_2} = 18 g/min; (f) *P*: 20 MPa, C_{feed}: 0.8 mg/mL, Q_{CO_2} = 54 g/min.

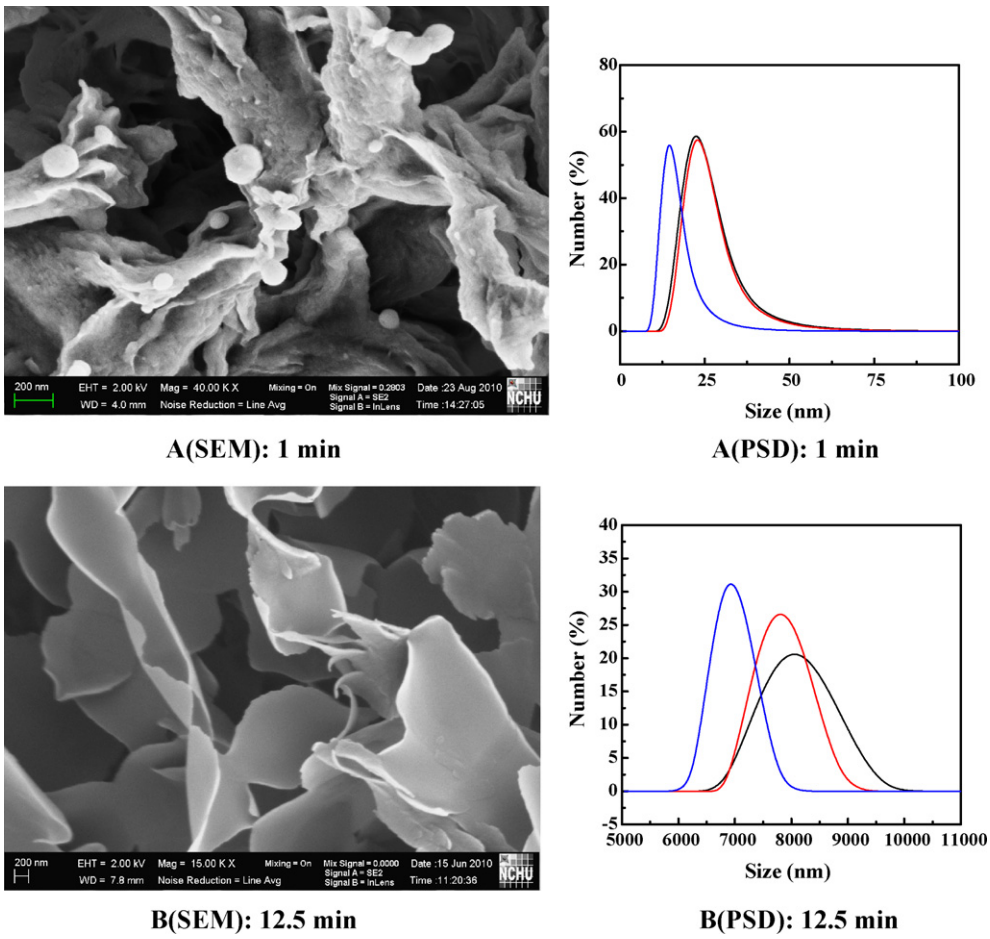

Fig. 4. Morphology (SEM) and particle size distribution (PSD) at different injection times. A: 1 min; B: 12.5 min. (P: 20 MPa, C_{feed}:0.4 mg/mL, Q_{CO_2} = 54 g/min, T: 313 K).

rich by utilization of the HPLC analysis, and were enhanced from 121.2 mg/g to 530.9 mg/g. We stopped the collection when high C_{zea} value was observed (F32) because there is only low C_{zea} value in fractions after F32. The F24–F32 portions consisting of 56.4% zeaxanthin were mixed to form materials having an average value of the C_{zea} = 436.2 mg/g (43.6%), which were then used as feeds for the SC-CO_2 anti-solvent processes.

3.4. Preliminary experimention of SC-CO_2 antisolvent precipitation

Prior to the study of a SAS process, solubilities of algal extracts in various solvents were crucial and had to be estimated for selection of suitable feed solutions. Table 3 shows experimental solubility data of algal extracts with different zeaxanthin contents in various solvents, which were obtained using visual observation of a fixed amount of solutes dissolved in the solvent. Further investigation into these solubilities shows chloromethane is the best solvent in which to dissolve the zeaxanthin-rich extracts. Good solvents (i.e. DCM) that easily dissolve zeaxanthin are not suitable for the purification of zeaxanthin in the SAS precipitation process. Ethanol and acetone are better solvents since their solubilities decrease sharply with increasing content of zeaxanthin in the extracts. Acetone was finally selected as a solvent to dissolve the algal extracts to form feed solutions for the SAS process study.

3.5. RSM-designed SC-CO_2 antisolvent precipitation

Response surface methodology (RSM) based on the center composite scheme for three design variables (pressure, feeding concentration and flow rate of CO_2) with seven axial points, seven factor points and one center point was employed for the SC-CO_2 antisolvent precipitation. The condition for the RSM-designed SC-CO_2 anti-solvent precipitation was set to 313 K. Table 4 lists experimental data concerning this RSM-designed at pressures ranging from 10 to 20 MPa, feeding concentrations from 0.4 to 0.8 mg/mL, and flow rates of CO_2 from 18 to 54 g/min. One major response of the concentration of zeaxanthin (C_{zea}) was analyzed using a quadratic regression model in the Design-Expert software package (Stat-Ease, Version 6.01). Fig. 2 which plots the three-dimensional response surfaces for the concentrations of zeaxanthin (C_{zea}) shows that the concentrations of zeaxanthin (C_{zea}) which represent the quality of precipitates changed with pressure, solution concentration and flow rate of CO_2 at the center point of P = 15 MPa, C_{feed} = 0.6 mg/g and Q_{CO_2} = 36 g/min. The concentrations of zeaxanthin (C_{zea}) increased as pressure and CO_2 flow rate increased, and it decreased as solution concentration increased from 0.4 to 0.8 mg/mL at high pressures. A quadratic regression model was determined from the F-test and the analysis of variance (i.e. $F_{Czea} = 5.77 > 4.77 = F$ (0.05, 9, 5), $R^2 = 0.91$ for Fig. 2). From the F-test, concentrations of zeaxanthin respond significantly in this RSM.

3.6. Morphology and particle size distribution

Fig. 3(a and b) displays the morphology of precipitate as they vary with pressure. The higher operating pressure produced a smaller size of flake-type precipitates. The degree of supersaturation increased as pressures increased above the critical point of the mixture; this was due to a decrease of solute concentration in the

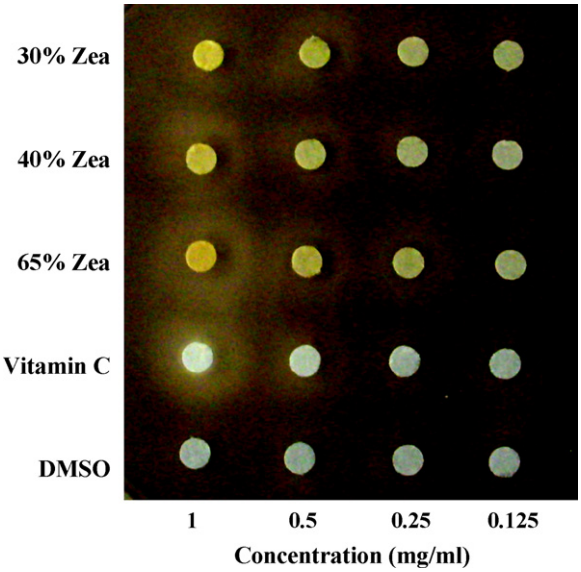

Fig. 5. Agar-plate-tyrosinase inhibition by column fractions and SC-CO_2 precipitates.

solution mixed with CO_2. Fig. 3(c and d) indicates solution concentrations increasing from 0.4 mg/mL to 0.8 mg/mL lead to an increase in the size of the snow flower-type precipitates due to a larger mass input. Fig. 3(e and f) shows that a thin size of the snow flower-type precipitates can be found in the experiments with high CO_2 flow rate. The reason may be that a high CO_2 flow rate is associated with rapid expansion of the feed solution and nucleation of the precipitates occurs in the well mixing of acetone and carbon dioxide. For a given degree of expansion, reducing the solution concentration of zeaxanthin promotes the supersaturation of the solute and the easy formation of narrow size precipitates. In contrast, increasing the solution concentration of zeaxanthin promotes the agglomeration of precipitates, such that the snow flower-type precipitates become large. In the study of classification of particulates in the SAS process, the experimental data of Fig. 4 indicates that reducing the injection time from 12.5 min to 1 min leads to nano-sized round-type precipitates, and it is obvious that a small mass input during a short injected time leads to nucleation during the SAS process only.

3.7. Agar-plate tyrosinase inhibition of SC-CO_2 antisolvent precipitation

An agar-plate model was adopted to evaluate the correlation between the zeaxanthin contents and tyrosinase inhibition by the algal extracts and the SAS precipitates. Fig. 5 shows that qualitative effect of the 65% zeaxanthin sample on the anti-tyrosinase activity is very close to that of Vitamin C, because that brighten area is almost identical at the dosed concentration of 1 mg/m1. The bright area and brightness representing the ability of anti-tyrosinase are in descending order of the 65% > 40% > 30% zeaxanthin samples. The inhibition of tyrosinase activity increased with the content of zeaxanthin in the samples.

4. Conclusions

This study successfully examined the generation of submicron-sized precipitates containing zeaxanthin from algal solutions of *Nannochloropsis oculata* using reverse-phase column elution chromatography coupled with the SAS precipitation process. Experimental results show that the amount of zeaxanthin in the column elution was 21-fold higher than that in the dry solid algae. A three center-composite factor of response surface method designed supercritical anti-solvent precipitations of the algal solutions was executed to find crucial operational parameters affecting the amount of zeaxanthin in the submicron sized precipitates. The results revealed that the concentration of feed solution and the flow rate of carbon dioxide are very important to influence the amount of zeaxanthin. Higher amounts of zeaxanthin in the precipitates can be found in the experiments of low feed concentrations. On the other hand, smaller sizes of the round-type particulates can be found in high CO_2 flow rates under a short injection time. This work demonstrates that supercritical carbon dioxide anti-solvent precipitation of the fraction obtained from the column elution chromatography substantially produces submicron-sized precipitates containing a large amount of zeaxanthin; the purest reached 67.4% by weight.

Acknowledgements

The authors would like to thank the National Science Council of the Republic of China, Taiwan for financially supporting this research (NSC98-2622-E005-004-CC1 and NSC98-2622-E005-016-CC3) and the Taichung Veterans General Hospital and National Chung Hsing University, Taiwan, for partially supporting under contract no. TCVGH-NCHU 977603.

References

[1] N. Krishnadev, A.D. Meleth, E.Y. Chew, Nutritional supplements for age-related macular degeneration, Current Opinion in Ophthalmology 21 (2010) 184–189.
[2] S.M. Moeller, P.F. Jacques, J.B. Blumberg, The potential role of dietary xanthophylls in cataract and age-related macular degeneration, Journal of the American College of Nutrition 19 (2000) 522S–527S.
[3] J.P. SanGiovanni, E.Y. Chew, T.E. Clemons, F.L. Ferris, G. Gensler, A.S. Linblad, R.C. Milton, J.M. Seddon, R.D. Sperduto, The relationship of dietary carotenoid and vitamin A, E, and C intake with age-related macular degeneration in a case–control study – AREDS Report no. 22, Archives of Ophthalmology 125 (2007) 1225–1232.
[4] P.S. Bernstein, F. Khachik, L.S. Carvalho, G.J. Muir, D.Y. Zhao, N.B. Katz, Identification and quantitation of carotenoids and their metabolites in the tissues of the human eye, Experimental Eye Research 72 (2001) 215–223.
[5] A. Telfer, S. Dhami, S.M. Bishop, D. Phillips, J. Barber, Beta-carotene quenches singlet oxygen formed by isolated photosystem II reaction centers, Biochemistry 33 (1994) 14469–14474.
[6] P. Horton, A. Ruban, Molecular design of the photosystem II light-harvesting antenna: photosynthesis and photoprotection 56 (2005) 365–373.
[7] K.K. Niyogi, Photoprotection revisited: genetic and molecular approaches, Annual Review of Plant Biology 50 (1999) 333–359.
[8] M. Havaux, K.K. Niyogi, The violaxanthin cycle protects plants from photooxidative damage by more than one mechanism, Proceedings of the National Academy of Sciences of the United States of America 96 (1999) 8762–8767.
[9] A.M. Gilmore, N. Mohanty, H.Y. Yamamoto, Epoxidation of zeaxanthin and antheraxanthin reverses nonphotochemical quenching of photosystem-II chlorophyll-a fluorescence in the presence of trans-thylakoid delta-ph, FEBS Letters 350 (1994) 271–274.
[10] B. Demmigadams, Carotenoids and photoprotection in plants – a role for the xanthophyll zeaxanthin, Biochimica et Biophysica Acta 1020 (1990) 1–24.
[11] B.C. Liau, C.T. Shen, F.P. Liang, S.E. Hong, S.L. Hsu, T.T. Jong, C.M.J. Chang, Supercritical fluids extraction and anti-solvent purification of carotenoids from microalgae and associated bioactivity, Journal of Supercritical Fluids (2010), doi:10.1016/j.supflu.2010.07.002.
[12] C.H. Chen, Y.H. Yang, C.T. Shen, S.M. Lai, C.M.J. Chang, C.J. Shieh, Recovery of vitamins B from supercritical carbon dioxide-defatted rice bran powder using ultrasound water extraction, Journal of Taiwan Institute of Chemical Engineers (2010) (in press).
[13] C.R. Chen, Y.N. Lee, M.R. Lee, C.M.J. Chang, Supercritical fluids extraction of cinnamic acid derivatives from Brazilian propolis and the effect on growth inhibition of colon cancer cells, Journal of Taiwan Institute of Chemical Engineers 40 (2009) 130–135.
[14] J. Fages, H. Lochard, J.J. Letourneau, M. Sauceau, E. Rodier, Particle generation for pharmaceutical applications using supercritical fluid technology, Powder Technology 141 (2004) 219–226.
[15] H.T. Wu, M.J. Lee, H.M. Lin, Nano-particles formation for pigment red 177 via a continuous supercritical anti-solvent process, Journal of Supercritical Fluids 33 (2005) 173–182.
[16] O.J. Catchpole, J.B. Grey, K.A. Mitchell, J.S. Lan, Supercritical antisolvent fractionation of propolis tincture, Journal of Supercritical Fluids 29 (2004) 97–106.
[17] C.J. Chang, A.D. Randolph, Precipitation of microsize organic particles from supercritical fluids, AIChE Journal 35 (1989) 1876–1882.

[18] K.X. Chen, X.Y. Zhang, J. Pan, W.C. Zhang, W.H. Yin, Gas antisolvent precipitation of ginkgo ginkgolides with supercritical CO_2, Powder Technology 152 (2005) 127–132.
[19] M.J. Cocero, S. Ferrero, Crystallization of beta-carotene by a GAS process in batch – effect of operating conditions, Journal of Supercritical Fluids 22 (2002) 237–245.
[20] F. Miguel, A. Martin, T. Gamse, M.J. Cocero, Supercritical anti-solvent precipitation of lycopene – effect of the operating parameters, Journal of Supercritical Fluids 36 (2006) 225–235.
[21] J.J. Wu, C.T. Shen, T.T. Jong, C.C. Young, H.L. Yang, S.L. Hsu, C.M.J. Chang, C.J. Shieh, Supercritical carbon dioxide anti-solvent process for purification of micronized propolis particulates and associated anti-cancer activity, Separation and Purification Technology 70 (2009) 190–198.
[22] C.R. Chen, C.T. Shen, J.J. Wu, S.L. Hsu, C.M.J. Chang, Precipitation of 3,5-diprenyl-4-hydroxycinnamic acid in Brazilian propolis from supercritical carbon dioxide solutions, Journal of Supercritical Fluids 50 (2009) 176–182.
[23] M. Rantakyla, M. Jantti, O. Aaltonen, M. Hurme, The effect of initial drop size on particle size in the supercritical antisolvent precipitation (SAS) technique, Journal of Supercritical Fluids 24 (2002) 251–263.
[24] C.M.J. Chang, A.D. Randolph, N.E. Craft, Separation of beta-carotene mixtures precipitated from liquid solvents with high-pressure CO_2, Biotechnology Progress 7 (1991) 275–278.
[25] L. Kao, C.R. Chen, C.M.J. Chang, Supercritical CO_2 extraction of turmerones from turmeric and high-pressure phase equilibrium of CO_2 + turmerones, Journal of Supercritical Fluids 43 (2007) 276–282.